INFLUENCE OF THE FIELD DIRECTION ON THE MAGNETIC PHASES OF A UNIAXIAL TWO-SUBLATTICE ANTIFERROMAGNET. I. GROUND STATE ENERGIES, CRITICAL FIELDS AND MAGNETIZATIONS

By G. Kozłowski

Institute for Low Temperature and Structure Research, Polish Academy of Sciences, Wrocław*

(Received January 29, 1971)

The influence of an external magnetic field of arbitrary direction on the zero-temperature magnetic phases of a two-sublattice uniaxial Néel-type antiferromagnet is studied in the nearest-neighbours spin-coupling approximation. In Part I, the approximate ground states (spin wave reference states) for the different magnetic phases are determined, and a critical-field diagram for the phase transitions is given. Strict solutions for the field-dependence of the direction of spin alignment in the sublattice reference states are obtained and discussed, and the magnetizations and ground state energies are calculated as functions of the external field. In Part II, the longitudinal and transversal magnetic susceptibilities in the different magnetic phases are derived, and the influence of the magnetic field strength and direction on those quantities is examined. The results are compared with experimental data and shown to justify the approximations of standard theories only in limiting cases.

1. Introduction

The problem of field-induced magnetic phases in uniaxial two-sublattice antiferromagnets is still subject to intensive theoretical and experimental investigations [1–4]. Earlier theoretical treatments [5–7], carried out within the framework of the molecular-field approximation (MFA), established the general features of these magnetic phases. More recently, magnetic phases in antiferromagnets have been treated using more sophisticated theoretical techniques [8–12]. However, the influence of a (homogeneous) external magnetic field of arbitrary direction on the magnetic phases has been studied in [7, 13] only, and then without determining the strict solutions for the field-dependence of the direction of spin-alignment in the sublattices. We shall show that for zero temperature ($T = 0$) such strict solutions can be obtained, and that in limiting cases they correspond to the approximate

* Address: Instytut Niskich Temperatur i Badań Strukturalnych, Polska Akademia Nauk, Wrocław, Plac Katedralny 1, Poland.

results of the MFA theory [7, 13]. Apart from the fact that our solutions permit us to extend the MFA considerations of the whole magnetic-field interval $0 \leqslant H < \infty$, they also enable us to apply the spin wave theory to all the magnetic phases, as the dependence of the spin wave energy spectrum on the external magnetic field can be effectively determined.

When employing the spin wave formalism to the Heisenberg model of ferro- or antiferromagnetism, there is usually the problem of choosing a suitable reference state (spin deviation vacuum) if the spin wave interactions are to be sufficiently small to justify the standard long-wavelength low-temperature approximations [14–18]. A typical example is the case when the (homogeneous) external magnetic field is not parallel to a direction of easiest magnetization, in which case the reference state depends on the field strength and direction. In [14, 17, 18], two different methods of determining the reference state for magnetic crystals have been studied quite generally: method A, which is preferably used in the theory of ferromagnetism [2], aims at determining the approximate ground state of the spin Hamiltonian, by minimizing its expectation value in a class of trial states generated by spatial rotations from the state of complete spin-alignment (saturation state); and method B, which resides in eliminating the terms linear with respect to the spin wave creation and annihilation operators appearing in the transformed Hamiltonian (see, *e. g.* [10, 11]). In [14, 17, 18], the methods A and B were shown to be equivalent, in a limited sense[1].

In determining the reference state of the two-sublattice uniaxial antiferromagnet with an external magnetic field of arbitrary direction, we apply the method A with the following restrictions:

a) the class of reference states is confined to "homogeneous" states corresponding to complete spin alignment in the sublattices (sublattice saturation state);

b) the antiferromagnet is assumed to be of Néel type, and the (exchange) interaction is restricted to nearest neighbours only;

c) uniaxial nearest-neighbour exchange anisotropy is assumed;

d) intra-atomic interaction (crystal-field anisotropy) is excluded.

Within these limitations, in Part I, strict solutions for the field-dependence of the direction of spin-alignment in the sublattice reference states are obtained and discussed for the different magnetic phases of the system. On this basis, the ground state energies and the longitudinal and transversal magnetizations are determined as functions of the field strenghts and direction. In Part II, the longitudinal and transversal magnetic susceptibility for each magnetic phase is derived and the influence of the field strength and direction on these quantities is examined. The results are compared with experimental data and are shown to justify the approximations of standard theories in limiting cases.

Our considerations are confined to $T = 0$, the case $T > 0$ will be examined in a subsequent paper.

---

[1] A third method of determining the reference state in the spin wave theory was introduced in [11] and shown to be equivalent to method B in the non-interacting-spin-waves approximation. The method A has recently been applied in examining the stability of homogeneous spin deviation reference states in uniaxial ferri- and antiferrimagnets with field parallel or perpendicular to the anisotropy axis [19, 20].

2. Determination of reference states and stability regions.

We consider a spin Hamiltonian of the form

$$\tilde{\mathscr{H}} = |J| \sum_{\langle f,g \rangle} (X\tilde{S}_f^x \tilde{S}_g^x + \tilde{S}_f^y \tilde{S}_g^y + Z\tilde{S}_f^z \tilde{S}_g^z) -$$

$$-\mu H^z \{\sum_f \tilde{S}_f^z + \sum_g \tilde{S}_g^z\} - \mu H^x \{\sum_f \tilde{S}_f^x + \sum_g \tilde{S}_g^x\} \tag{1}$$

where $X = 1+|K_x/J|$, $Z = 1+|K_z/J|$, $(Z > X)$. The subscripts f, g denote respectively the sites of the first and second sublattice (each of them having $N/2$ sites); $\langle f, g \rangle$ denotes the summation over nearest neighbours; K_x, K_z are the exchange anisotropy constants in the x and z directions, respectively, and J is the nearest-neighbour exchange integral between atoms belonging to different sublattices; μ is the effective magnetic moment per lattice atom; $H_x = H \cos \xi$, $H_z = H \sin \xi$ $(0 \leqslant \xi \leqslant \pi/2)$ denote the components of the homogeneous external magnetic field respectively in the x and z direction.

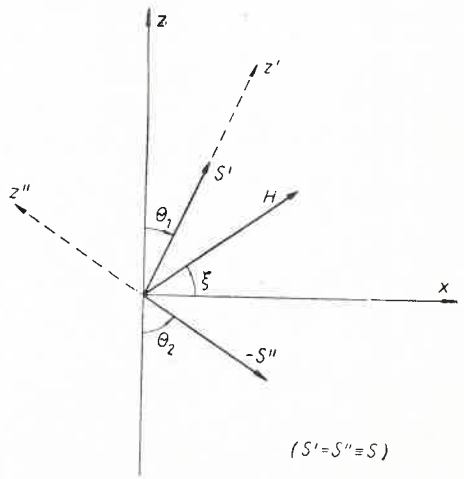

Fig. 1

Similarly as in [14, 19], we perform the following rotations of the spins in the plane $x0z$;

$$\begin{aligned}
&\tilde{S}_f^x = S_f^x \cos \Theta_1 + S_f^z \sin \Theta_1 \qquad \tilde{S}_g^x = S_g^x \cos \Theta_2 - S_g^z \sin \Theta_2 \\
&\tilde{S}_f^y = S_f^y \qquad\qquad\qquad\qquad \tilde{S}_g^y = S_g^y \\
&\tilde{S}_f^z = -S_f^x \sin \Theta_1 + S_f^z \cos \Theta_1 \quad S_g^z = \tilde{S}_g^x \sin \Theta_2 + S_g^z \cos \Theta_2.
\end{aligned} \tag{2}$$

(This actually corresponds to introducing two different coordinate systems, (x', y, z') and (x'', y, z''), in the respective sublattices, as illustrated in Fig. 1. For simplicity, however, we omit the primes and double-primes in Eq. (2) and in the following.)

Furthermore, we define the sublattice saturation states $|0\rangle_f$ and $|0\rangle_g$ (homogeneous spin-deviation reference states; cp. [14]) as follows:

$$S_f^z|0\rangle = S|0\rangle, \quad S_f^+|0\rangle = 0$$
$$S_g^z|0\rangle = -S|0\rangle, \; S_g^-|0\rangle = 0 \tag{3}$$

where

$$S_{f,g}^+ = S_{f,g}^x + iS_{f,g}^y, \; |0\rangle = |0>_f \cdot |0\rangle_g, {}_f\langle 0|0\rangle_f = {}_g\langle 0|0\rangle_g = 1$$

Subsequently, the stable reference state (*i. e.*, the aproximate ground state of the system) is determined by minimizing the mean value of the transformed Hamiltonian in the state $|0\rangle$ with respect to the parameters Θ_1 and Θ_2,

$$\min \langle 0|H|0\rangle \equiv \min E_0(\Theta_1, \Theta_2). \tag{4}$$

By taking into account Eqs (1)—(4) we obtain for E_0 the expression

$$E_0(\Theta_1, \Theta_2) = -\alpha\{Z\cos\Theta_1\cos\Theta_2 - X\sin\Theta_1\sin\Theta_2 + h\sin(\Theta_1+\xi) + h\sin(\Theta_2-\xi)\} \tag{5}$$

where $\alpha = 1/2\, S^2 N|J|$, $h = \mu H/\gamma_0 S|J|$, and γ_0 is the number of nearest neighbours.

We obtain the stable reference states and the stability regions by solving the necessary and examining the sufficient conditions for the existence of a minimum of E_0 as a function of two variables Θ_1, Θ_2 and four parameters X, Z, h, ξ:

$$\frac{\partial E_0}{\partial \Theta_1} = \frac{\partial E_0}{\partial \Theta_2} = 0; \; \Delta = \frac{\partial^2 E_0}{\partial \Theta_1^2}\cdot\frac{\partial^2 E_0}{\partial \Theta_2^2} - \left(\frac{\partial^2 E_0}{\partial \Theta_1 \partial \Theta_2}\right)^2 > 0, \; \frac{\partial^2 E_0}{\partial \Theta_1^2} > 0. \tag{6}$$

The necessary conditions can be written in the form

$$Z\sin\Theta_2\cos\Theta_1 + X\cos\Theta_2\sin\Theta_1 = h\cos(\Theta_2-\xi), \tag{7}$$

$$Z\cos\Theta_2\sin\Theta_1 + X\sin\Theta_2\cos\Theta_1 = h\cos(\Theta_1+\xi). \tag{8}$$

Multiplying Eqs (7) and (8) by Z and X, respectively, and subtracting (7) from (8) we obtain:

$$(Z^2-X^2)\sin\Theta_2\cos\Theta_1 = hZ\cos(\Theta_2-\xi) - hX\cos(\Theta_2+\xi). \tag{9}$$

The same procedure, with Z and X interchanged, leads to

$$(Z^2-X^2)\cos\Theta_2\sin\Theta_1 = hZ\cos(\Theta_1+\xi) - hX\cos(\Theta_2-\xi). \tag{10}$$

Upon squaring and subtracting again the above equations, one obtains

$$\sin\Theta_2(a\sin\Theta_2 - b\cos\Theta_2) = \sin\Theta_1(a\sin\Theta_1 + b\cos\Theta_1) \tag{11}$$

where

$$a = Z^2 - X^2 + h^2\cos 2\xi, \quad b = h^2\sin 2\xi. \tag{12}$$

Adding Eqs (7) and (8) we obtain a second equation,

$$\cos\frac{\Theta_2+\Theta_1}{2}\left[(Z+X)\sin\frac{\Theta_2+\Theta_1}{2}-h\cos\left(\xi-\frac{\Theta_2-\Theta_1}{2}\right)\right]=0 \tag{13}$$

which, together with Eq. (11), permits us to obtain easily an explicit form for the dependence of the angles Θ_1 and Θ_2 on the strength (h) and direction (ξ) of the magnetic field.

Indeed, it can readily be seen from Eq. (11) that, in the case $a>0$, one has

$$\cos(2\Theta_2-\vartheta)=\cos(2\Theta_1+\vartheta),\ \operatorname{tg}\vartheta=\frac{b}{a} \tag{14}$$

with the condition

$$h^2\cos 2\xi+Z^2-X^2\equiv F(h,\xi)\geqslant 0 \tag{15}$$

which restricts the field strength h according to its direction ξ (or *vice versa*). (Note that ϑ is a function of h and ξ, cp. Eq. (12).) Taking into account that Eq. (14) implies

$$\Theta_2=\Theta_1+\vartheta+\pi k \tag{16}$$

or

$$\Theta_2=-\Theta_1+\pi k \tag{17}$$

where $k=0,\pm1,\pm2,\ldots$, we obtain from Eq. (13) two possible solutions:

$$\cos\left(\Theta_1+\frac{\vartheta+\pi k}{2}\right)=0 \tag{18}$$

$$\sin\left(\Theta_1+\frac{\vartheta+\pi k}{2}\right)=\frac{h}{Z+X}\cos\left(\xi-\frac{\vartheta+\pi k}{2}\right) \tag{19}$$

for the case (16), and the solution

$$\cos\left(\Theta_1+\xi-\frac{\pi k}{2}\right)=0 \tag{20}$$

in the case (17).

The inequivalent solutions (for $a>0$) following from (16)—(20) are g ven in Table I.

As indicated in Table I, there are only three stable solutions, and even these are confined to certain stability regions (apart from the restriction (15)) that follow from the minimum conditions (6).

For the first solution,

$$\Theta_1=\frac{\pi}{2}-\frac{\vartheta}{2};\ \Theta_2=\frac{\pi}{2}+\frac{\vartheta}{2}, \tag{21}$$

the inequalities in (6) have the form

$$\Delta=\alpha^2\left\{h\cos\left(\xi-\frac{\vartheta}{2}\right)+(Z-X)\cos\vartheta\right\}\left\{h\cos\left(\xi-\frac{\vartheta}{2}\right)-(Z+X)\right\}>0, \tag{22}$$

$$\frac{\partial^2 E_0}{\partial\Theta_1^2}=-\alpha\left\{Z\sin^2\frac{\vartheta}{2}+X\cos^2\frac{\vartheta}{2}-h\cos\left(\xi-\frac{\vartheta}{2}\right)\right\}>0 \tag{23}$$

TABLE I

$a > 0$	k	Solution	Stability
$\cos\left(\Theta_1+\frac{\vartheta+\pi k}{2}\right)=0$ $\Theta_2=\Theta_1+\vartheta+\pi k$	0	$\Theta_1=\frac{\pi}{2}-\frac{\vartheta}{2};\Theta_2=\frac{\pi}{2}+\frac{\vartheta}{2}$	stable
		$\Theta_1=\frac{3\pi}{2}-\frac{\vartheta}{2};\Theta_2=\frac{3\pi}{2}+\frac{\vartheta}{2}$	unstable
	1	$\Theta_1=-\frac{\vartheta}{2};\Theta_2=\pi+\frac{\vartheta}{2}$	
		$\Theta=\pi-\frac{\vartheta}{2};\Theta_2=2\pi+\frac{\vartheta}{2}$	
$\sin\left(\Theta_1+\frac{\vartheta+\pi k}{2}\right)=$ $=\frac{h}{Z+X}\times$ $\times\cos\left(\xi-\frac{\vartheta+\pi k}{2}\right)$ $\Theta_2=\Theta_1+\vartheta+\pi k$	0	$\sin\left(\Theta_1+\frac{\vartheta}{2}\right)=\frac{h}{Z+X}\cos\left(\xi-\frac{\vartheta}{2}\right),$ $\Theta_2=\Theta_1+\vartheta$	stable
	1	$\cos\left(\Theta_1+\frac{\vartheta}{2}\right)=\frac{h}{Z+X}\sin\left(\xi-\frac{\vartheta}{2}\right),$ $\Theta_2=\Theta_1+\vartheta+\pi$	unstable
$\cos\left(\Theta_1+\xi-\frac{\pi k}{2}\right)=0$ $\Theta_2=-\Theta_1+\pi k$	0	$\Theta_1=\frac{\pi}{2}-\xi;\Theta_2=-\frac{\pi}{2}+\xi$	stable
		$\Theta_1=\frac{3\pi}{2}-\xi;\Theta_2=-\frac{3\pi}{2}+\xi$	
	1	$\Theta_1=\pi-\xi;\Theta_2=\xi$	unstable
		$\Theta_1=2\pi-\xi;\Theta_2=-\pi+\xi$	

and lead to the (additional) field restriction (cp. (15))

$$h\cos\left(\xi-\frac{\vartheta}{2}\right)-(Z+X)\equiv F'(h,\xi)\geqslant 0. \tag{24}$$

For the second solution,

$$\sin\left(\Theta_1+\frac{\vartheta}{2}\right)=\frac{h}{Z+X}\cos\left(\xi-\frac{\vartheta}{2}\right);\ \Theta_2=\Theta_1+\vartheta, \tag{25}$$

one obtains the stability conditions

$$\Delta=\alpha^2\cos^2\left(\Theta_1+\frac{\vartheta}{2}\right)\sqrt{(Z^2-X^2+h^2\cos 2\xi)^2+(h^2\sin 2\xi)^2}>0, \tag{26}$$

$$\frac{\partial^2 E_0}{\partial\Theta_1^2}=\alpha\left\{Z\cos^2\frac{\vartheta}{2}+X\sin^2\frac{\vartheta}{2}+h\sin\left(\xi-\frac{\vartheta}{2}\right)\cos\left(\Theta_1+\frac{\vartheta}{2}\right)\right\}>0 \tag{27}$$

and the field restriction

$$F'(h, \xi) \leqslant 0 \tag{28}$$

with F' as defined by Eq. (24). The third solution,

$$\Theta_1 = \frac{\pi}{2} - \xi, \quad \Theta_2 = -\frac{\pi}{2} + \xi \text{ or } \Theta_1 = \frac{3\pi}{2} - \xi, \quad \Theta_2 = -\frac{3\pi}{2} + \xi, \tag{29}$$

is stable if

$$\Delta = \alpha^2\{-(Z^2-X^2)\cos 2\xi - h^2\} > 0, \tag{30}$$

$$\frac{\partial^2 E_0}{\partial \Theta_1^2} = \alpha\{Z \sin^2 \xi + X \cos^2 \xi + h\} > 0, \tag{31}$$

which implies

$$(X^2-Z^2)\cos 2\xi - h^2 \equiv F'''(h, \xi) \geqslant 0,$$

$$\pi/4 < \xi \leqslant \pi/2. \tag{32}$$

To obtain the solutions for $a < 0$, let us note that in this case Eq. (12) implies instead of (15) the restriction

$$F(h, \xi) \leqslant 0, \quad (\pi/4 < \xi \leqslant \pi/2) \tag{33}$$

in which case Eq. (11) leads to the equation

$$\cos(2\Theta_2 + \vartheta') = \cos(2\Theta_1 - \vartheta'), \ \mathrm{tg}\,\vartheta' = -\frac{b}{a}. \tag{34}$$

One easily verifies that the only stable solutions of Eqs (13) and (34) have the form (21) and (25), with the substitution

$$\vartheta \to \pi - \vartheta' \tag{35}$$

and the additional field restrictions (apart from (33))

$$h \sin\left(\xi + \frac{\vartheta'}{2}\right) - (Z+X) \equiv F''(h, \xi) \geqslant 0 \tag{36}$$

$$F''(h, \xi) \leqslant 0 \tag{37}$$

corresponding respectively to the cases (21) and (25).

3. Critical-field diagram and stable spin configurations

The stability regions in the (h, ξ) -plane of the five solutions given above are schematically shown in Fig. 2. The boundaries of these regions follow from the equations

$$F(h, \xi) = F'(h, \xi) = F''(h, \xi) = F'''(h, \xi) = 0 \tag{38}$$

and are respectively denoted by $h_c(\xi)$), $h_c'(\xi)$, $h_c''(\xi)$ and $h_c'''(\xi)$. Thus, the solutions (21) and (29), with ϑ as defined by Eqs (14) and (12), correspond respectively to the regions *2*

and *3* in Fig. 2, while the solution (25) extends over the regions *1* and *3*. The solutions (21) and (25), but with the substitution (35) and ϑ' as defined by (34), are respectively ascribed to the regions *2'* and *1'*.

One easily verifies that the solutions in the regions *1* and *1'* describe a canted-spin configuration (*CS*), whereas those in the regions *2* ans *2'* correspond to a ferromagnetic

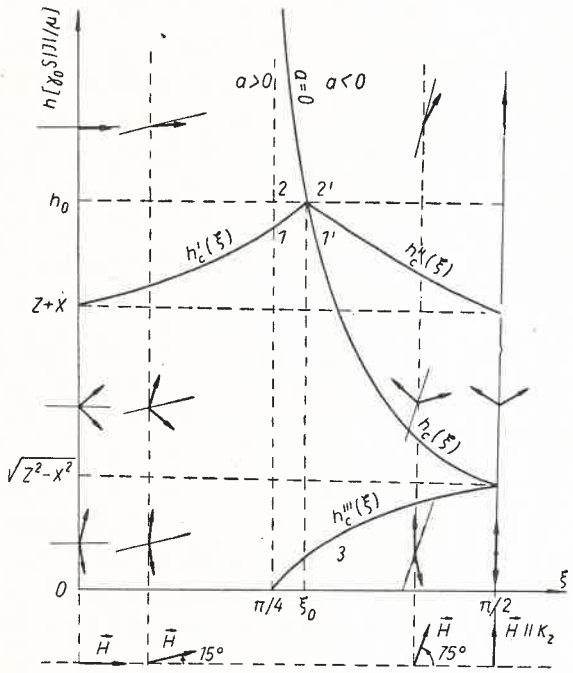

Fig. 2

spin-alignment (*F*); *i.e.*, the spins are parallel to each other but n o t to the external magnetic field, except in the extreme cases when $\xi = 0$ (field perpendicular to anisotropy axis), or $\xi = \pi/2$ (field parallel to anisotropy axis), or $h = \infty$ for arbitrary ξ, as in this case

$$\vartheta, \vartheta' \to 2\xi \quad \text{for} \quad h \to \infty \tag{39}$$

according to Eqs (12), (14) and (34). Hence, it is only in the extreme cases $\xi = 0$ and $\xi = \pi/2$ when paramagnetism at finite fields occurs (in the conventional sense). Note that in the *CS*-regions *1* and *1'* the spins belonging to different sublattices form the same angle with the field-direction only in the extreme cases $\xi = 0$ ($\Theta_1 = \Theta_2$) and $\xi = \pi/2$ ($-\Theta_1 = \pi - \Theta_2$; standard spin-flop phase). In the region *3*, we actually have two stable solutions, (25) and (29), of which the former is simply the *CS*-solution of region *1*, whereas the latter corresponds to an antiferromagnetic configuration (*AF*) along the field-direction and, as will be shown below, represents a metastable phase. For $\xi = \pi/2$, these two solutions coincide. The above discussed spin configurations in the respective stability regions are indicated in Figs 2 and 3.

One easily proves that, except for (25) and (29) on the boundaries $h = 0$ and $h_c'''(\xi)$, the solutions of neighbouring regions coincide at the boundaries $h_c(\xi)$, $h_c'(\xi)$ and $h_c''(\xi)$, and that for $h < Z+X$ in the CS configuration the spins belonging to different sublattices lie on opposite sides of the field, while for $h > Z+X$ and $0 < \xi < \pi/2$ they lie on the

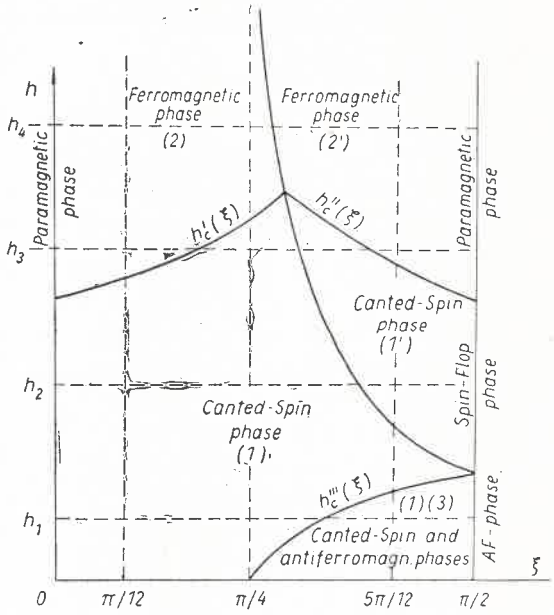

Fig. 3

same side but, surprisingly, at larger angles to the anisotropy direction than the field itself (in the CS as well as in the F configuration). Indeed, it is readily seen from (25) that

$$\Theta_1 = \pi/2-\xi, \quad \Theta_2 = \pi/2+\vartheta-\xi \tag{40}$$

for $h = Z+X$, which means that at this field strength the sublattice spins S' in Fig. 1 pass through the field direction (the same holds for the case (35)).

The field strengths $h = Z+X$ for $\xi = 0$ and $\xi = \pi/2$, and $h = \sqrt{Z^2-X^2}$ for $\xi = \pi/2$ correspond respectively to the standard critical fields for the $CS \leftrightarrow P$ and $AF \leftrightarrow CS$ phase transitions [3, 4, 10–12, 19, 20]. It is seen from Fig. 2 that, if these phase transitions exist for $0 < \xi < \pi/2$, they should respectively correspond to a $CS \leftrightarrow F$ phase transition at the boundaries $h_c'(\xi)$ and $h_c''(\xi)$, and to some kind of $CS \leftrightarrow CS$ phase transition at the boundary $h_c(\xi)$ between the CS regions *1* and *1'*. In either case, the corresponding critical field strengths should increase with increasing field-declination from the directions $\xi = 0$ and $\xi = \pi/2$, reaching its maximum value

$$h_0 = (Z+X)\sqrt{1+\frac{1}{4}\left(\frac{Z-X}{Z+X}\right)^2} \tag{41}$$

at the angle (cp. Fig. 2)

$$\xi_0 = \pi/4 + \operatorname{arctg}\left(\frac{1}{2}\frac{Z-X}{Z+X}\right). \tag{42}$$

Beyond that, there is the boundary $h_c'''(\xi)$ between the AF (metastable) and CS (stable) configuration, and $h_c(\xi)$ between the regions *2* and *2'* which also might correspond to some kind of $F \leftrightarrow F$ phase transition.

We shall show below and in Part II of this paper that, for $0 < \xi < \pi/2$ and $T = 0$, there is no (magnetic) phase transition whatever on the whole curve $h_c(\xi)$, that the boundaries $h_c'(\xi)$ and $h_c''(\xi)$ correspond to a second-order $CS \leftrightarrow F$ phase transition, and that a first-order $AF \leftrightarrow CS$ phase transition occurs at the boundary $h_c'''(\xi)$. (Note that, instead of $h_c'(\xi)$, $h_c''(\xi)$ and $h_c'''(\xi)$ one can use as well the inverse functions $\xi_c'(h)$, $\xi_c''(h)$ and $\xi_c'''(h)$ which determine the critical field direction for each phase transition as a function of the field strength.)

4. Ground state energies and magnetizations

In order to determine what kind of phase transitions — if any — take place at the boundaries $h_c(\xi)$, $h_c'(\xi)$, $h_c''(\xi)$ and $h_c'''(\xi)$, we examine the ground state energy E_0, the magnetization and, in Part II, the susceptibility of the system in the particular stability regions. Upon inserting the solutions (25), (21) and (29) for $a > 0$ into (5) we obtain for the spin configurations CS, F and AF respectively the ground state energies

$$E_0^{CS} = -\alpha\left\{Z\cos^2\frac{\vartheta}{2} + X\sin^2\frac{\vartheta}{2} + \frac{h^2}{Z+X}\cos^2\left(\xi - \frac{\vartheta}{2}\right)\right\}, \tag{43}$$

$$E_0^{F} = -\alpha\left\{-Z\sin^2\frac{\vartheta}{2} - X\cos^2\frac{\vartheta}{2} + 2h\cos\left(\xi - \frac{\vartheta}{2}\right)\right\}, \tag{44}$$

$$E_0^{AF} = -\frac{\alpha}{2}\{Z+X-(Z-X)\cos 2\xi\}. \tag{45}$$

For the case $a < 0$ (regions *1'* and *2'* in Fig. 2), Eqs (43) and (44) are valid when replacing ϑ by ϑ' according to Eq. (35).

With the components of the sublattice magnetizations in the (approximate) ground state (3) defined as follows

$$M_{\mathrm{I}}^z = \mu\sum_f \langle 0|\tilde{S}_f^z|0\rangle, \quad M_{\mathrm{I}}^x = \mu\sum_f \langle 0|\tilde{S}_f^x|0\rangle \tag{46}$$

$$M_{\mathrm{II}}^z = \mu\sum_g \langle 0|\tilde{S}_g^z|0\rangle, \quad M_{\mathrm{II}}^x = \mu\sum_g \langle 0|\tilde{S}_g^x|0\rangle \tag{47}$$

the zero-temperature components of the total (reduced) magnetization in the direction perpendicular ($m^{\perp}$) and parallel ($m^{\parallel}$) to the external magnetic field, and its length m have

the form:

$$m^{\perp} = m^z \cos\xi - m^x \sin\xi = -\sin\frac{\Theta_2+\Theta_1}{2}\sin\left(\xi-\frac{\Theta_2-\Theta_1}{2}\right) \tag{48}$$

$$m^{||} = m^z \sin\xi + m^x \cos\xi = \sin\frac{\Theta_2+\Theta_1}{2}\cos\left(\xi-\frac{\Theta_2-\Theta_1}{2}\right) \tag{49}$$

$$m = \sqrt{(m^{\perp})^2+(m^{||})^2} = \sin\frac{\Theta_2+\Theta_1}{2} \tag{50}$$

where $m^z = (M_{\mathrm{I}}^z+M_{\mathrm{II}}^z)/\mu NS$, $m^x = (M_{\mathrm{I}}^x+M_{\mathrm{II}}^x)/\mu NS$.

From (48)–(50) and (21), (25) and (29) we obtain for the respective stability regions the magnetizations

$$m_F^{\perp} = -\sin\left(\xi-\frac{\vartheta}{2}\right);\ m_F^{||} = \cos\left(\xi-\frac{\vartheta}{2}\right);\ m_F = 1 \tag{51}$$

$$m_{CS}^{\perp} = -\frac{1}{2}\frac{h}{Z+X}\sin(2\xi-\vartheta);\ m_{CS}^{||} = \frac{h}{Z+X}\cos^2\left(\xi-\frac{\vartheta}{2}\right);$$

$$m_{CS} = \frac{h}{Z+X}\cos\left(\xi-\frac{\vartheta}{2}\right) \tag{52}$$

$$m_{AF}^{\perp} = m_{AF}^{||} = m_{AF} = 0. \tag{53}$$

For the case $a < 0$ the respective quantities follow from Eqs (51), (52) upon substituting (35).

The above formulae permit us to obtain analytical expressions for the values of the quantities E_0, $m^{||}$, $m^{\perp}$ and m at the boundaries of the stability regions, by inserting the respective critical-field curves $h_c(\xi)$, $h_c'(\xi)$, $h_c''(\xi)$ and $h_c'''(\xi)$ following from Eq. (38). The results are given in Appendix A. As is seen from Eqs (A16)–(A18), there is a first-order phase transition between the phases AF and CS along the boundary $h_c'''(\xi)$. Since $E_0^{AF} > E_0^{CS}$ in the whole region *3* (except for $\xi = \pi/2$), the AF phase is to be regarded as metastable. One easily proves that $E_0^{AF} = E_0^{CS}$ for $\xi = \pi/2$, as in this case $\vartheta = 0$.

As regards the remaining boundaries, it is seen from Appendix A that all the examined quantities are continuous and hence no first-order magnetic phase transitions occur in this case. It will be shown in Part II that no magnetic phase transitions of any order take place along the whole boundary $h_c(\xi)$, and that the boundaries $h_c'(\xi)$ and $h_c''(\xi)$ correspond to second-order phase transitions.

5. Discussion of results

To illustrate quantitatively the dependence of the system's ground state energy and magnetization in the different magnetic phases on the strength and direction of the external magnetic field, schematic numerical curves for $X = 1$ ($K_x = 0$) and $Z = 1.1$ ($K_z = 0.1|J|$) are given in Figs 4–11, for four values of the external-field strength ($h = h_1, h_2, h_3, h_4$) and five different field directions ($\xi = 0°, 15°, 45°, 75°, 90°$), as indicated in Fig. 3 (dashed straight lines).

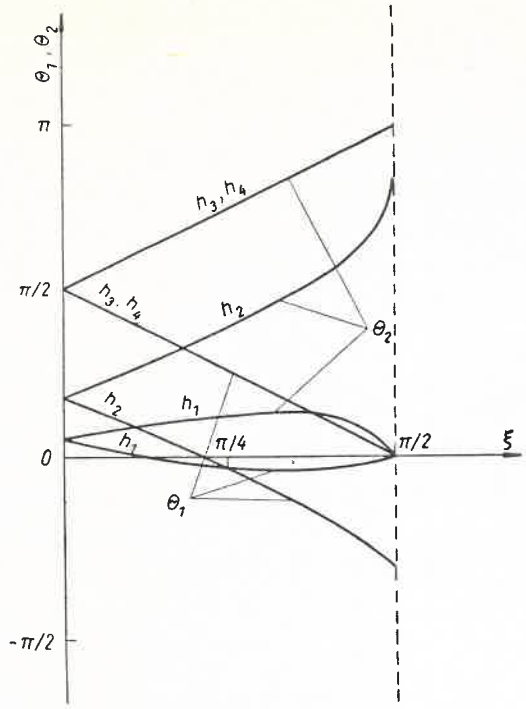
Θ_1, Θ_2
π
$\pi/2$
0
$-\pi/2$
h_3, h_4
h_3, h_4
h_2
h_2
h_1
h_1
Θ_2
Θ_1
$\pi/4$
$\pi/2$
ξ

Fig. 4

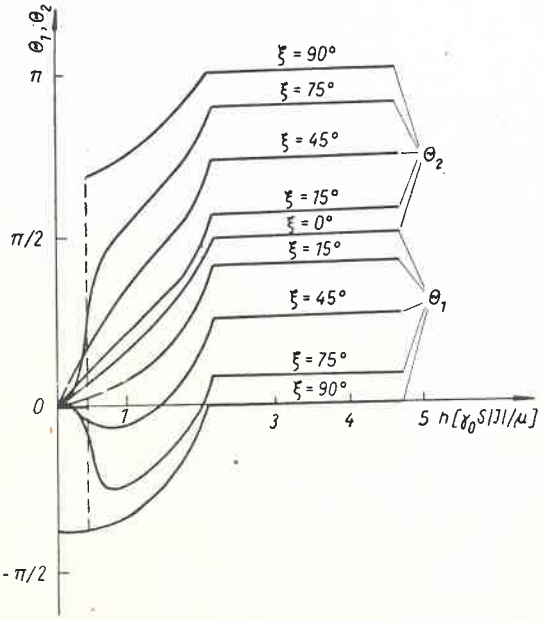
Θ_1, Θ_2
π
$\pi/2$
0
$-\pi/2$
$\xi = 90°$
$\xi = 75°$
$\xi = 45°$
$\xi = 15°$
$\xi = 0°$
$\xi = 15°$
$\xi = 45°$
$\xi = 75°$
$\xi = 90°$
Θ_2
Θ_1
1
3
4
5 $h[\gamma_0 S(3)/\mu]$

Fig. 5

The ferromagnetic solution (21) and the canted-spin solution (25) (regions *2* and *1* in Figs 2, 3), as well as their counterparts following from the substitution (35) (regions *2'* and *1'* in Figs 2, 3) are shown in Fig. 4 as functions of the field direction ξ for four fixed field strengths, and in Fig. 5 as functions of the field strength for five fixed field directions. The antiferromagnetic (metastable) solution (29) (region *3* in Figs 2, 3) is not illustrated, as it is a linear function of the field direction ξ and independent of the field strength. The curves for h_3 in Fig. 4 differ only slightly from those for h_4 (which is not indicated on the plot), namely, for field angles ξ corresponding in Fig. 3 to the canted-spin configuration

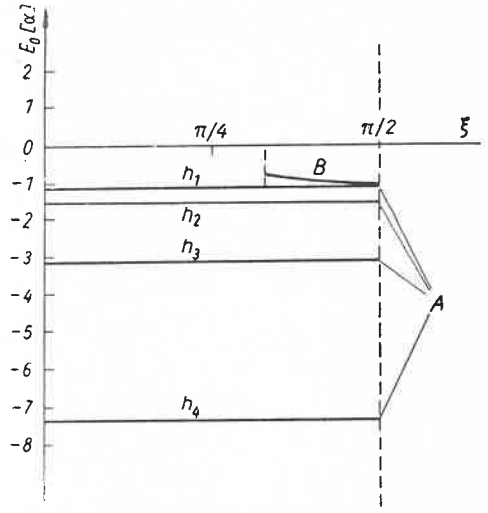

Fig. 6

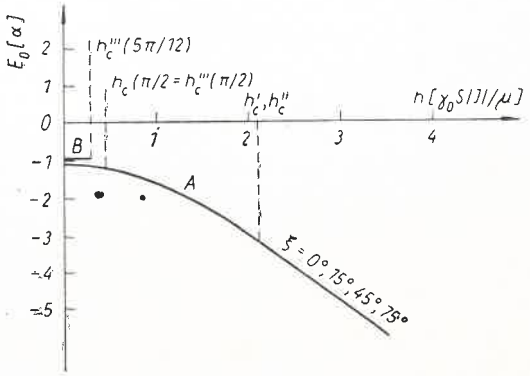

Fig. 7

interval between the critical-field curves $h_c'(\xi)$ and $h_c''(\xi)$. In Fig. 5, the dashed vertical line indicates the discontinuity of the solution for the longitudinal-field case ($\xi = \pi/2$) corresponding to the first-order antiferromagnetic-spin-flop phase transition at the critical field strength $h_c'''(\pi/2)$. Also, the curve in Fig. 5 flatten off in the ferromagnetic regions *2* and *2'* (for

$h > h_c'(\xi)$ or $h > h_c''(\xi)$, respectively), approaching for $h \to \infty$ and $0 < \xi < \pi/2$ the asymptotic values $\Theta_1 = \pi/2 - \xi$ and $\Theta_2 = \pi/2 + \xi$ (complete spin-alignment in field direction). It is plainly seen from Fig. 5 that the first derivatives of the solutions are discontinuous at the critical-field curves $h_c'(\xi)$ and $h_c''(\xi)$, which indicates the existence of a second-order $CS \leftrightarrow F$ phase transition (cp. Part II of this paper).

It is worth-while noting that for fields inclined to the anisotropy axis, the spin S' which forms a smaller angle with the field direction (cp. Fig. 1) undergoes within the CS-phase a swing-back motion similar to that in antiferrimagnets (see [19, 20]). This effect does not vanish until the external field is almost perpendicular to the anisotropy axis (cp. the curves Θ_1 in Fig. 5).

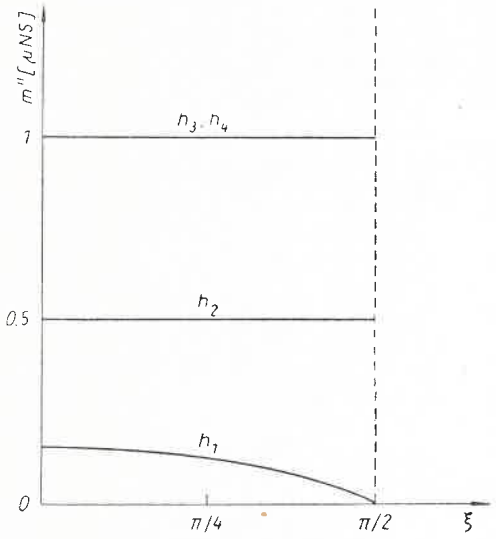

Fig. 8

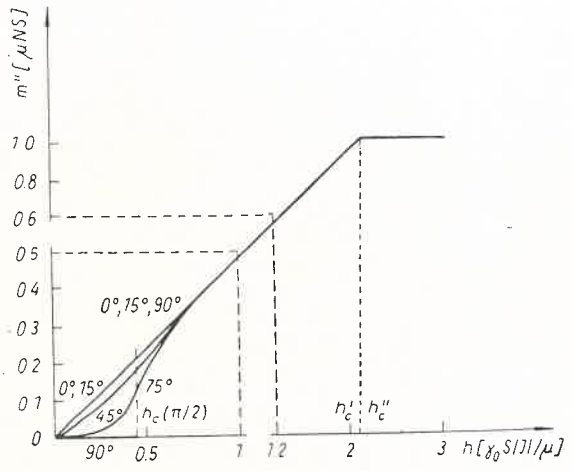

Fig. 9

The ground-state-energy and the components of the total magnetization along ($m^{\parallel}$) and perpendicular ($m^{\perp}$) to the external magnetic field, corresponding respectively to the curves in Figs 4 and 5, are shown in Figs 6–11. In Figs 6 and 7, besides the energy curves A corresponding to the solutions in Figs 4 and 5 there are in addition the curves B corresponding to the metastable AF-solution (29) plotted respectively for fixed $h = h_1$ and $\xi = 5\pi/12$ (cp. dashed lines in region *3* in Fig. 3).

It is seen from Figs 6 and 7 that the energy curves A are continuous and practically independent of the field direction ξ (regardless of the magnetic phase), as the slight increase with increasing ξ of the curves A in Fig. 6 is hardly discernible (with increasing ξ the curve A in Fig. 7 shifts slightly upwards, its AF-part in the interval $0 \leqslant h \leqslant h_c(\pi/2)$ being constant for $\xi = 90°$). A possible first-order $AF-CS$ phase transition is also visible in Figs 6 and 7.

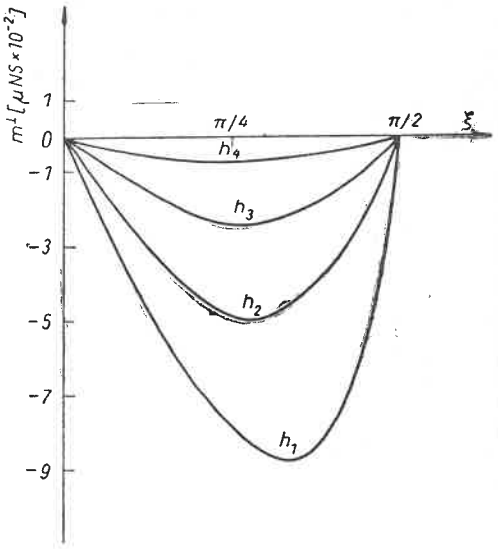

Fig. 10

From Figs 10 and 11 the (negative) transversal magnetization component is clearly seen to have a maximum for a specific field direction at constant field strength (Fig. 10), and for $h = h_c(\pi/2)$ at constant field direction (Fig. 11). The maximum of $-m^{\perp}$ in Fig. 10 evidently shifts to $\xi = \pi/2$ and tends to zero as $h \to \infty$. From Eq. (52) it is readily seen that the same holds for $h \to 0$. In the case of fixed field direction, Fig. 10, the maximum of $-m^{\perp}$ at $h_c(\pi/2)$ vanishes, too, for $\xi \to 0$ and tends to $\sqrt{(Z-X)/4(Z+X)}$ for $\xi \to \pi/2$ while $m^{\perp} \to 0$ for $h \neq h_c(\pi/2)$, $\xi \to \pi/2$ (discontinuity). Note, however, that $m^{\perp} = 0$ for $\xi = \pi/2$ and $h \to h_c(\pi/2)$, according to Eq. (52).

The influence of the field direction and field strength on the longitudinal magnetization is shown in Figs 8 and 9, of which the latter illustrates perhaps best the transition of the system from the double-phase to the triple-phase case while changing the field direction from that of the hardest ($\xi = 0$) to that of the easiest ($\xi = \pi/2$) magnetization. Since for small declinations of the field from these extreme directions the longitudinal component $m^{\parallel}$ is practically equal to the length m of the total magnetization as defined by Eq. (50) (note the difference

of the units in Figs 9 and 11), the experimental results reported in [21] agree quite reasonably with the curves in Fig. 9. Our results permit us also easily extend the molecular-field calculations given in [5, 6] beyond the restrictions assumed by those authors.

It should be noted that the curves $m^{\parallel}$ for $0 < \xi < \pi/2$ and $h > h_c(\pi/2)$ lie actually somewhat below the uppermost straight curves for $\xi = 0$ and $\pi/2$, which is not indicated in Fig. 9 (except for $h_c(\pi/2) < h \lesssim 0.8$). For $h \to \infty$, these curves approach gradually their

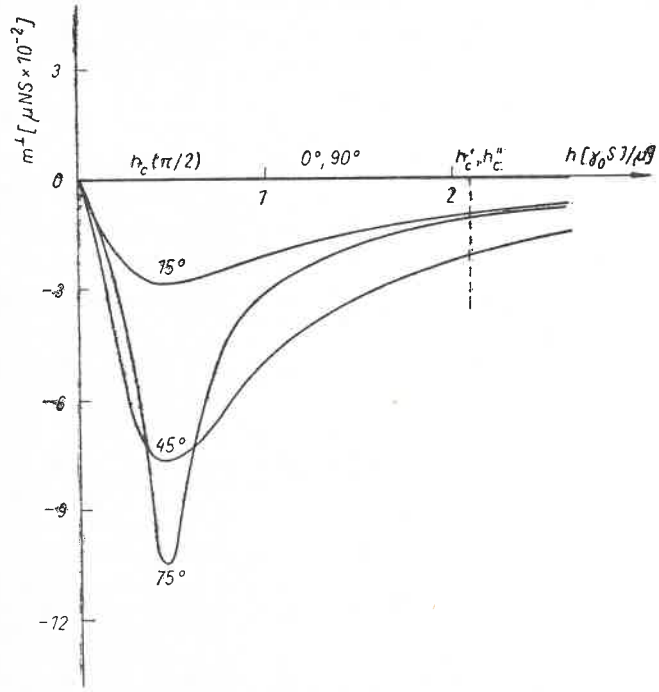

Fig. 11

asymptotic value $m^{\parallel} = 1$ which coincides with the saturation value for $\xi = 0$ and $\pi/2$ in the paramagnetic region $h \geqslant h_c'(0) = h_c''(\pi/2) = Z+X$ (cp. Figs 2 and 11).

No magnetization curves are provided for the AF-solution from region *3* (Fig. 2) as in this case $m^{\perp} = m^{\parallel} = m = 0$ according to Eq. (53).

Numerical curves of the components of the magnetic susceptibility tensor, corresponding to those given here for the ground state energy and magnetization, will be presented and discussed in Part II.

The author wishes to thank Dr W. J. Ziętek for helpful discussions concerning this work and for reading the manuscript.

APPENDIX A

From Eqs (43)–(45), (51) and (52) one easily obtains the limiting values of the respective quantities when approaching the boundaries $h_c(\xi)$, $h_c'(\xi)$, $h_c''(\xi)$ and $h_c'''(\xi)$ of the stability regions following from Eq. (38). Hence, for the critical-field curves $h_c'(\xi)$ and $h_c''(\xi)$ between

the *CS* (*1*, *1'*) and *F*(*2*, *2'*) spin configuration regions (cp. Figs 2 and 3) we get

$$E_0^{CS}|_{h=h_c^i(\xi)} = E_0^{F}|_{h=h_c^i(\xi)} = -\alpha\left\{Z+X+Z\cos^2\frac{\delta^i}{2}+X\sin^2\frac{\delta^i}{2}\right\}, \tag{A1}$$

$$m_{CS}^{\parallel}|_{h=h_c^i(\xi)} = m_F^{\parallel}|_{h=h_c^i(\xi)} = \cos\left(\xi-\frac{\delta^i}{2}\right), \tag{A2}$$

$$m_{CS}^{\perp}|_{h=h_c^i(\xi)} = m_F^{\parallel}|_{h=h_c^i(\xi)} = -\sin\left(\xi-\frac{\delta^i}{2}\right), \tag{A3}$$

$$m_{CS}|_{h=h_c^i(\xi)} = m_F|_{h=h_c^i(\xi)} = 1 \tag{A4}$$

where the superfix i stands for the prime or double-prime mark, and

$$\delta^i = \begin{cases}\vartheta & \text{for} \quad h_c^i = h_c'(\xi)\\ \vartheta & \text{for} \quad h_c^i = h_c''(\xi).\end{cases} \tag{A5}$$

(Note that, according to Eqs (12), (14) and (34), the angles ϑ and ϑ' are themselves functions of the external magnetic field.)

Similarly, we obtain for the lower part of the $h_c(\xi)$ boundary (between the *CS*-regions *1* and *1'*) the values

$$E_0^{CS}(1)|_{h=h_c(\xi)} = E_0^{CS}(1')|_{h=h_c(\xi)} = -\frac{\alpha}{2}\left\{Z+X-(Z-X)\operatorname{ctg}\left(\frac{\pi}{4}-\xi\right)\right\}, \tag{A6}$$

$$m_{CS}^{\perp}(1)|_{h=h_c(\xi)} = m_{CS}^{\perp}(1')|_{h=h_c(\xi)} = -R/2, \tag{A7}$$

$$m_{CS}^{\parallel}(1)|_{h=h_c(\xi)} = m_{CS}^{\parallel}(1')|_{h=h_c(\xi)} = -R\operatorname{ctg}\left(\frac{\pi}{4}-\xi\right)\Big/2, \tag{A8}$$

$$m_{CS}(1)|_{h=h_c(\xi)} = m_{CS}(1')|_{h=h_c(\xi)} = -R/2\sin(\pi/4-\xi), \tag{A9}$$

and for the upper part of this boundary (between the *F*-regions *2* and *2'*) the values

$$E_0^{F}(2)|_{h=h_c(\xi)} = E_0^{F}(2')|_{h=h_c(\xi)} = -\alpha\{-(Z+X)/2+\sqrt{2(X^2-Z^2)\operatorname{ctg}(\pi/4-\xi)}\}, \tag{A10}$$

$$m_F^{\perp}(2)|_{h=h_c(\xi)} = m_F^{\perp}(2')|_{h=h_c(\xi)} = \sin(\pi/4-\xi), \tag{A11}$$

$$m_F^{\parallel}(2)|_{h=h_c(\xi)} = m_F^{\parallel}(2')|_{h=h_c(\xi)} = \cos(\pi/4-\xi), \tag{A12}$$

$$m_F(2)|_{h=h_c(\xi)} = m_F(2')|_{h=h_c(\xi)} = 1 \tag{A13}$$

where

$$R = \sqrt{\frac{X-Z}{X+Z}}\cos 2\xi.$$

Finally, for the $h_c'''(\xi)$ boundary of the *AF*-region *3* we have

$$E_0^{AF}|_{h=h_c'''(\xi)} = -\frac{\alpha}{2}\{Z+X-(Z-X)\cos 2\xi\} \tag{A14}$$

and Eq. (53), while on the same curve $h_c'''(\xi)$ the respective quantities corresponding to the *CS* spin configuration (regions *1* and *3* in Figs 2 and 3) are continuous and assume the values

$$E_0^{CS}|_{h=h_c'''(\xi)} = -\frac{\alpha}{2}\{Z+X-\sqrt{2}\,(Z-X)\sin(\pi/4-2\xi)\}, \tag{A15}$$

$$m_{CS}^{\perp}|_{h=h_c'''(\xi)} = -R/2, \tag{A16}$$

$$m_{CS}^{\parallel}|_{h=h_c'''(\xi)} = R/2, \tag{A17}$$

$$m_{CS}|_{h=h_c'''(\xi)} = R/\sqrt{2}. \tag{A18}$$

REFERENCES

[1] Landolt-Börnstein, *Group III, Vol. 4*: Magnetic and other properties of oxides and related compounds; Springer Verlag, Berlin—Heidelberg—New York 1970.

[2] S. V. Tyablikov, *Methods of the Quantum Theory of Magnetism* (in Russian), Nauka, Moscow 1966.

[3] F. Keffer, *Spin Waves*, in: *Handbuch der Physik*, Vol. 18, Springer Verlag, Berlin—New York 1966.

[4] G. T. Rado, H. Suhl, *Magnetism*, Vol. **1**, Academic Press, New York and London 1963.

[5] J. S. Smart, *Effective Field Theories of Magnetism*, W. B. Saunders Co., Philadelphia 1966.

[6] L. Néel, *C.R. Acad. Sci.* (France) **5**, 232 (1936); T. Nagamiya, *Progr. Theor. Phys.*, **6**, 342, 350 (1951); K. Yosida, *Progr. Theor. Phys.*, **6**, 691 (1951).

[7] T. Nagamiya, K. Yosida, R. Kubo, *Advances in Phys.*, **4**, Part I, 6 (1955).

[8] P. W. Anderson, *Phys. Rev.*, **86**, 694 (1952); R. Kubo, *Phys. Rev.*, **87**, 568 (1952).

[9] H. Falk, *Phys. Rev.*, **133**, A1382 (1964); F. B. Anderson, H. B. Callen, *Phys. Rev.*, **136**, A1068 (1964).

[10] J. Feder, E. Pytte, *Phys. Rev.*, **168**, 140 (1968).

[11] A. Pękalski, W. J. Ziętek, *Acta Phys. Polon.*, **A39**, ... (1971).

[12] A. Pękalski, *Acta Phys. Polon.*, **A39**, ... (1971).

[13] H. Rohrer, H. Thomas, *J. Appl. Phys.*, **40**, 1025 (1969).

[14] H. Pfeiffer, W. J. Ziętek, *Acta Phys. Polon.*, **A38**, 176 (1970).

[15] W. J. Ziętek, *Acta Phys. Polon.*, **35**, 799 (1969); **36**, 145 (1969).

[16] A. Pękalski, W. J. Ziętek, *Acta Phys. Polon.*, **31**, 131 (1967).

[17] L. Biegała, *Acta Phys. Polon.*, **A38**, 773 (1970).

[18] H. Pfeiffer, *Acta Phys. Polon.*, **A39**, 209, 213 (1971).

[19] G. Kozłowski, L. Biegała, S. Krzemiński, *Acta Phys. Polon.*, **A39**, 417 (1971).

[20] S. Krzemiński, *Acta Phys. Polon.*, **A39**, 661 (1971).

[21] I. S. Jacobs, *J. Appl. Phys.*, **32**, Suppl. 61 (1961).